

Automatic target recognition using 3D passive sensing and imaging with independent component analysis

Cuong Manh Do^{*a}, Raúl Martínez-Cuenca^b and Bahram Javidi^a

^aDepartment of Electrical & Computer Engineering, University of Connecticut, 371 Fairfield Road U-2157, Storrs, Connecticut 06269-2157 USA

^bDepartment of Optics, University of Valencia, Calle Doctor Moliner 50, E46100 Burjassot, Spain

ABSTRACT

We present an overview of a method using Independent Component Analysis (ICA) and 3D Integral Imaging (II) technique to recognize 3D objects at different orientations. This method has been successfully applied to the recognition and classification of 3D scenes.

Keywords: Pattern recognition, 3D imaging, independent component analysis

1. INTRODUCTION

Three-dimensional (3D) object recognition¹⁻⁴ provides improved performance compared to the 2D algorithms. In this paper, we present an overview of 3D object recognition method by applying the ICA to the integral images.⁵

The integral imaging (II) is a 3D imaging technique which is especially easy to implement since it works naturally with incoherent light. In this technique, the 3D information is acquired by taking a photo of the scene through a microlens array (MLA)⁶⁻⁹. This procedure provides an integral image of the 3D object, i. e., a set of elemental images storing different perspectives of the 3D scene. The ICA was first proposed in the early 1990s¹⁰⁻¹³, and it has been applied whenever it is mandatory to determine the signals that compound an observable magnitude with no a priori knowledge of the sources. This technique has been extensively used in the field of digital image processing¹⁴⁻¹⁸. In this keynote paper, we present an overview of 3D object recognition using integral imaging and ICA pre-processing of data. In our scheme, Principle Component Analysis is applied as a preprocessing method to reduce the number of dimensions of the problem. Then, a kurtosis maximization-based ICA algorithm is applied⁵.

This paper is organized as follows. First, in Section 2, we introduce the description of both the integral imaging and the algorithm for the recognition of 3D scenes from the integral images. Next, Section 3 aims at the experimental results to demonstrate the performance of the proposed method. Finally we conclude in Section 4.

2. APPLICATION OF THE FAST ICA TO THE INTEGRAL IMAGING

As stated in the introduction, we use II to record the 3D information of the scenes. The procedure to capture an integral image is depicted in Fig. 1. Actually, the experimental implementation of the integral imaging is more elaborated, given that it evolves the use of telecentric-relay systems for a correct recording of the integral image with a digital camera. However, for the purposes of the current paper it is not necessary to specify the details about this procedure¹⁹. Note that, in our case, the object is put on a turnable stage to permit the acquisition of 3D information in a wider range of angles.

The elemental images are processed to perform the recognition. Fig. 2 shows the classification system using PCA-ICA. The acquired elemental sets are randomly permuted and used partially for training, the rest of them are used for testing. Column data vectors are made from elemental images for processing facility. Eigenvectors are calculated based on covariance decomposition using the training set. As a result, m eigenvectors with highest eigenvalues are chosen as PCA transform to project the data vectors to a lower dimension domain which keeps the most variance. Projected training vectors are used as inputs to ICA training algorithm. This preprocessing using PCA significantly reduces the number of dimensions of the data; and it also reduces the amount of time needed to train the ICA transform²⁰.

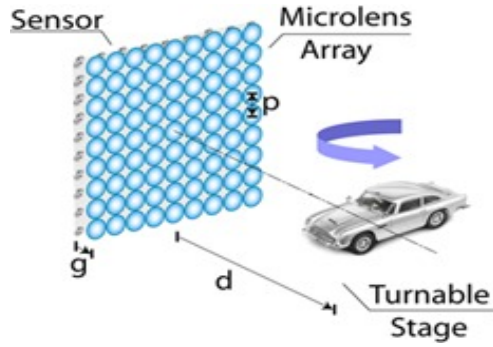


Fig. 1. Experimental optical set up for 3D integral imaging; P is the lens pitch.

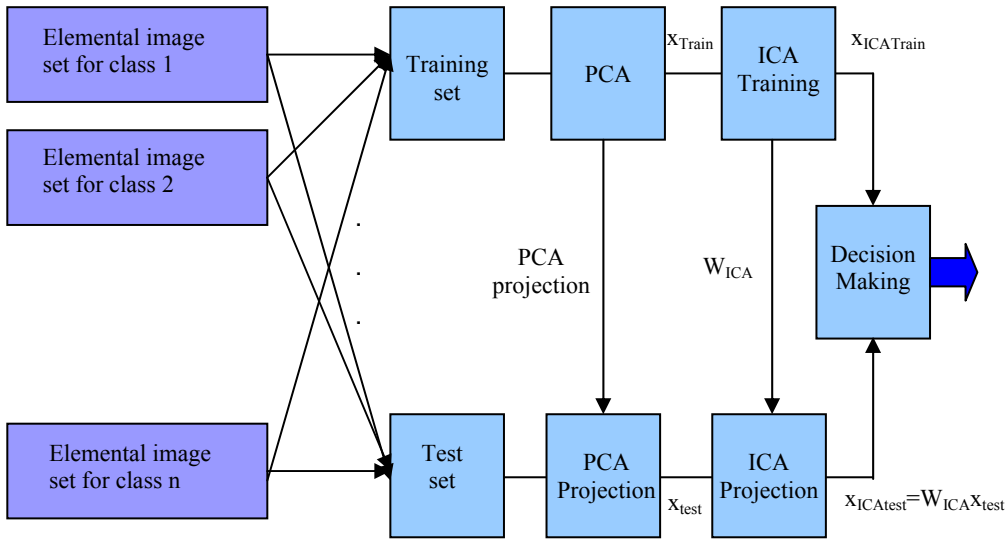


Fig. 2. Diagram of 3D integral imaging system for object recognition using ICA algorithm.

To understand how ICA algorithm works, let us define a data vector, $x = [x_1, x_2, \dots, x_n]^T$, and a vector of d statistically independent components, $s = [s_1, s_2, \dots, s_d]^T$, where $d \leq n$. The ICA states that any data vector x can be synthesized by linearly combining the independent components¹³, i. e.,

$$x = As, \quad (1)$$

where A denotes the so-called mixing matrix.

To calculate un-mixing matrix $W_{ICA} = A^{-1}$, we choose a kurtosis-maximization based ICA algorithm. Kurtosis of a variable y is defined as:

$$kurt(y) = E\{y^4\} - 3(E\{y^2\})^2 \quad (2)$$

In this equation, E denotes the expectation operator. As a consequence, the kurtosis of a Gaussian random variable is zero while it is non-zero for non-gaussian random variables. The data is first processed to obtain a whitened data vector, z ¹³

$$z = D^{-1/2}U^T x, \quad (3)$$

where $D=diag(d_1...d_n)$ is the diagonal matrix of the eigenvalues of the covariance matrix $E(xx^T)$ and $U=(u_1...u_n)$ is the eigenvector matrix.

Let w be a row in the transform matrix W_{ICA} , the fast-fixed point algorithm uses the kurtosis to find the direction of w so that $y=w^Tz$ is maximally non-gaussian, or correspondingly $kurt(w^Tz)$ is maximal in an iterative approach¹³, being

$$w \leftarrow E\left\{z\left(w^Tz\right)^3\right\}-3w, \quad (4)$$

the scheme for each iteration. Note that y becomes one independent component when the algorithm converges. We repeat the algorithm to attain different independent components and the ICA transform W_{ICA} .

The projection of a vector x in ICA domain is achieved using the estimated transform acquired in the training process, W_{ICA} . Note that x is a projected vector in PCA domain.

$$x_{ICA} = W_{ICA}x \quad (5)$$

Finally, the classification decision is based on the cosine c of the angle between the testing projected vectors and the training projected vector. High values of cosine mean high similarity. The class label of the testing projected vector is decided to be that of the training projected vector with which the cosine value is minimal:

$$c = \frac{x_{ICAtest}x_{ICAtrain}}{\|x_{ICAtest}\|\|x_{ICAtrain}\|} \quad (6)$$

where $x_{ICAtest}$, $x_{ICAtrain}$ are the representations of a testing and a training vector in ICA domain. Similarity is obtained with maximal cosine value. The class is determined as the class in which a training projected vector has the maximal cosine with the test projected vector.

3. EXPERIMENTAL SETUP AND RESULTS

We have performed some experiments to demonstrate the performance of our method. In the first one, we try to distinguish between 6 different objects; each object is a toy car approximately $25\text{ mm} \times 25\text{ mm} \times 45\text{ mm}$ in size (see Fig. 3(a)). Each car is rotated in order to capture the integral images at every 3° from -18° to $+18^\circ$ using a squared-grid micro-lens array of 3 mm focal length and 1 mm pitch. The car is located approximately 100 mm away from the micro-lens array.



Fig. 3. (a) A sample car object used in our experiments (b) Cropped sets of 6x5 integral images of one of the cars used in the experiments. Each elemental image is composed of 73 x 73 pixels.

A set of 6×5 elemental images is selected from each integral image (see Fig. 3(b)). We randomly choose ten out of thirty elemental images for training purposes, then use the rest of them are used for testing our procedure. The size of each elemental image is 73×73 pixels. Each elemental image is converted to a 5329×1 sized column vector to facilitate the processing. There are 780 vectors for training purposes and 1560 test vectors since there are 6 toy cars rotated at 13 angles. 100 attributes which retain the most variance are selected using PCA and used for ICA algorithm. Several basis images in the columns of matrix A are shown in Fig. 4.

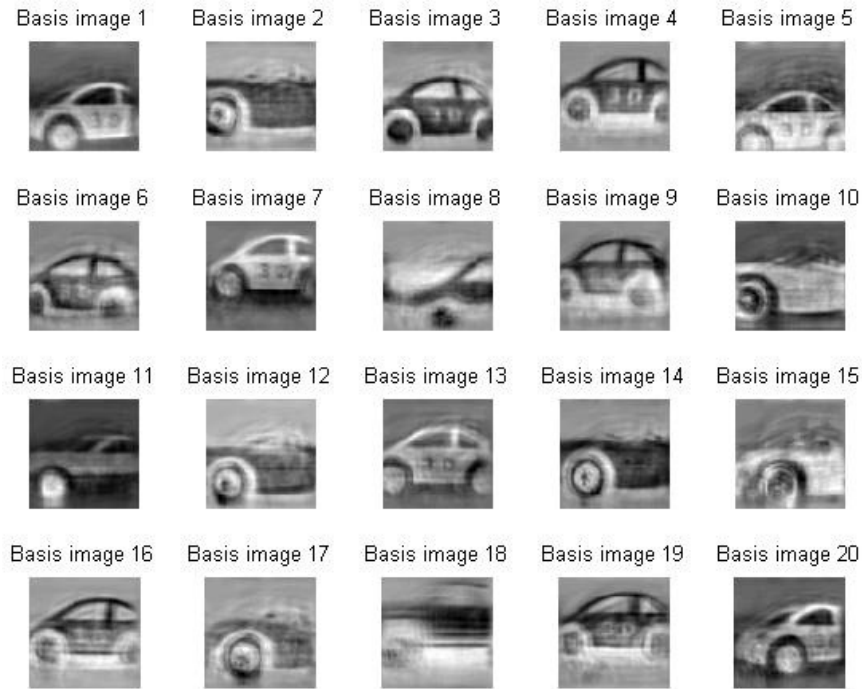


Fig. 4. First 20 basis images in columns of matrix A (or row of matrix W)

Figure 5 illustrates the classification rate for each class. We can observe that samples from class 2 are perfectly classified, whereas samples from classes 4 and 6 have lower correct rates of approximately 97%. The average rate for all classes is 98.4%. Figure 6 shows that samples from class 6 are most mis-classified at the angle of -18° , samples from class 4 are most mis-classified at the angles between -15° and -13° .

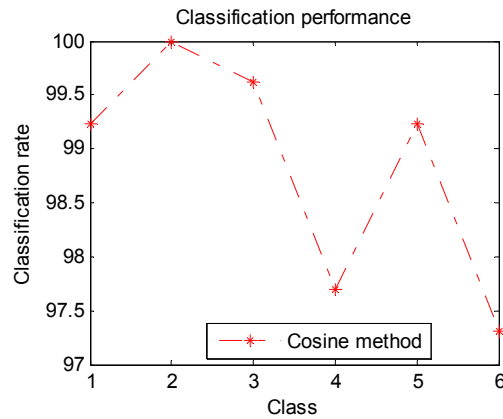


Fig. 5. Correct classification rate for toy car object classes from 1 to 6.

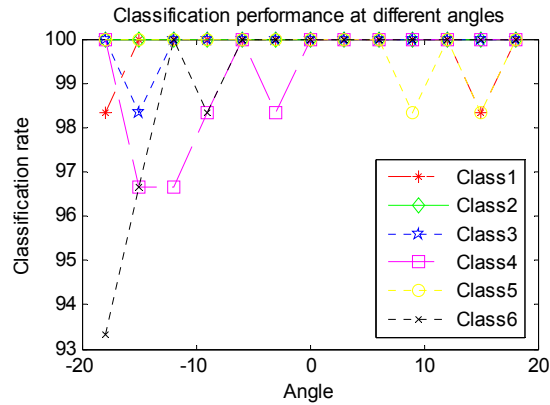


Fig. 6. Correct classification rate for toy car object classes from 1 to 6. The car orientation angles vary from -18° to 18° .

The training sample size plays an important role in getting the high correct classification rate (See Fig.7). We get a very high correct rate of 97% using a training data set of 10 randomly selected elemental images which are corresponding to 780 training vectors. Using 20 out of 30 elemental images which are corresponding to 1560 training vectors provides perfect classification result. The performance is lower when smaller sample sizes are used.

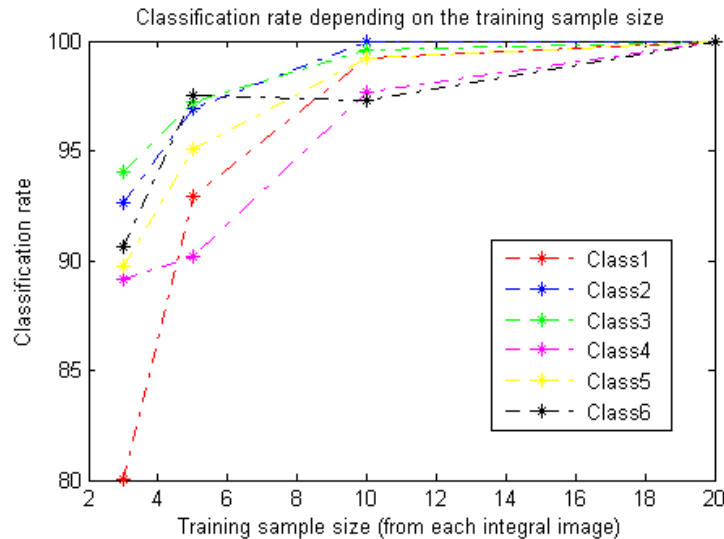


Fig. 7. Correct classification rate for different toy car object classes. Sample sizes of 234, 390, 780, 1560, corresponding to 3, 5, 10, 20 elemental images from each integral image, are used for training, respectively.

As a second experiment, we demonstrate that it is possible to distinguish between two car objects partially occluded by tree leaves (the corresponding elemental images are shown in Fig. 8). A higher level of occlusion is applied to the green car. Fig. 9 illustrates the correct classification result. We noted that using just 20 out of 30 elemental images provides almost perfect classification results. The correct classification rate still retains high for classes 4 and 6 if the training sample size for each integral image reduces to 5 or 10.



Fig. 8. Two integral images of occluded car object for toy car class 4 and toy car class 6, where the class #6 object car is heavily occluded.

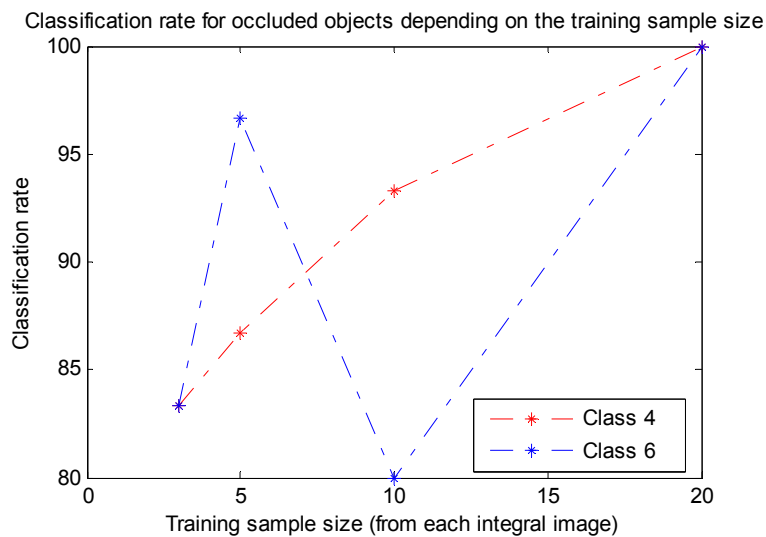


Fig. 9. Correct classification rate of classifying occluded car objects. Sample sizes of 234, 390, 780, 1560, corresponding to 3, 5, 10, 20 elemental images from each integral image, are used for training, respectively.

4. CONCLUSIONS AND REMARKS

We have presented an overview of a 3D object recognition method which combines integral imaging and kurtosis maximization-based ICA. The 3D information of a set of different objects has been captured at different angles by means of the integral imaging technique. We have demonstrated that it is possible to use the elemental images for training and testing the recognition system. In addition, the speed of the ICA algorithm has been improved thanks to the application of PCA to the original data prior to the ICA. The performance of our approach has been evaluated for different classes, angles and training sample sizes. Finally, some experiments with partially occluded objects have been carried out. Our results demonstrate that the system works fine with both non-occluded and occluded objects.

REFERENCES

- [1] Frauel, Y. and Javidi, B., "Digital three-dimensional image correlation by use of computer-reconstructed integral imaging," *Appl. Opt.* 41, 5488-5496 (2002).
- [2] Kishk and Javidi, B., "Improved resolution 3D object sensing and recognition using time multiplexed computational integral imaging," *Optics Express* 11, 3528-3541 (2003).

- [3] Yeom, S. and Javidi, B., "Three-dimensional distortion-tolerant object recognition using integral imaging," *Opt. Express* 12, 5795-5809 (2004).
- [4] Wu, C., Aggoun, A., McCormick, M., Kung, S. Y., "Depth measurement from integral images through viewpoint image extraction and a modified multibaseline disparity analysis algorithm," *J. Electr. Imaging* 14, 023018 (2005)
- [5] Do, C. M., Martínez-Cuenca, R. and Javidi, B., "Three-dimensional object-distortion-tolerant recognition for integral imaging using independent component analysis," *J. Opt. Soc. Am. A* 26, 245-251 (2009)
- [6] Lippmann, G., "La photographie integrale," *C. R. Acad. Sci.* 146, 446-451 (1908).
- [7] Okano, F., Hoshino, H., Arai, J. and Yayuma, I., "Real time pickup method for a three-dimensional image based on integral photography," *Appl. Opt.* 36, 1598-1603 (1997).
- [8] Martínez-Corral, M., Javidi, B., Martínez-Cuenca, R. and Saavedra, G., "Multifacet structure of observed reconstructed integral images," *J. Opt. Soc. Am. A* 22, 597-603 (2005).
- [9] Stern, A. and Javidi, B., "Three-dimensional image sensing, visualization, and processing using integral imaging," *Proceedings of the IEEE* 94, 591- 607 (2006).
- [10] Dubois, F., "Automatic spatial frequency selection algorithm for pattern recognition by correlation," *Appl. Opt.* 32, 4365-4371 (1993)
- [11] Farid, H. and Adelson, E. H., "Separating reflections from images by use of independent component analysis," *J. Opt. Soc. Am. A* 16, 2136-2145 (1999).
- [12] Hyvärinen, A., Hoyer, P. O. and Oja, E., "Sparse Code Shrinkage: Denoising by Nonlinear Maximum Likelihood Estimation", In *Advances in Neural Information Processing Systems 11 (NIPS1998)*, (MIT Press, 1999), pp. 473-479.
- [13] Hyvärinen, A., Karhunen, J. and Oja, E., *Independent Component Analysis*, John Wiley & Sons, New York (2001).
- [14] Der, S., Chan, A., Nasrabadi, N. and Kwon, H., "Automated vehicle detection in forward-looking infrared imagery," *Appl. Opt.* 43, 333-348 (2004).
- [15] Mahalanobis, A., "A review of correlation filters and their application for scene matching," in *Optoelectronic Devices and Systems for Processing*, B. Javidi, K. M. Johnson, eds. (SPIE Press, 1996), pp. 240-260.
- [16] Tsumura, N., Haneishi, H., and Miyake, Y., "Independent component analysis of skin color image," *J. Opt. Soc. Am. A* 16, 2169-2176 (1999).
- [17] Bartlett, M. S., Movellan, J. R. and Sejnowski, T. J., "Face recognition by independent component analysis," *IEEE Transactions on Neural Networks* 13, 1450-64 (2002)
- [18] Zheng, H., Huang, D. S., Shang, L., "Feature selection in independent component subspace for microarray data classification", *Neurocomputing*, Volume 69, Issue 16-18, 2407-2410 (2006)
- [19] Martínez-Cuenca, R., Navarro, H., Saavedra, G., Javidi, B., Martínez-Corral, M., "Enhanced viewing-angle integral imaging by multiple-axis telecentric relay system," *Opt. Express* 15, 16255-16260 (2007)
- [20] Murakami, H., and Kumar, B., "Efficient Calculation of Primary Images from a Set of Images", *IEEE Trans. Pattern Analysis and Machine Intelligence*, vol. PAMI-4, No. 5 (1982)